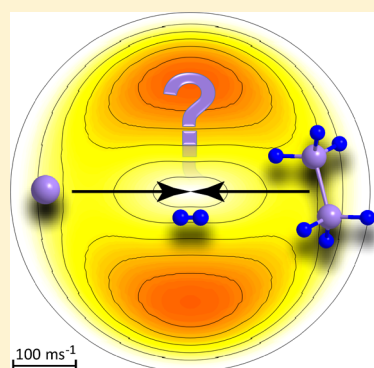


Gas-Phase Synthesis of the Elusive Trisilicontetrahydride Species ( $\text{Si}_3\text{H}_4$ )Tao Yang,<sup>†</sup> Beni B. Dangi,<sup>†,||</sup> Aaron M. Thomas,<sup>†</sup> Ralf I. Kaiser,<sup>\*,†,||</sup> Bing-Jian Sun,<sup>‡</sup> Monika Staś,<sup>§</sup> and Agnes H. H. Chang<sup>\*,‡</sup><sup>†</sup>Department of Chemistry, University of Hawai'i at Manoa, Honolulu, Hawaii 96822, United States<sup>‡</sup>Department of Chemistry, National Dong Hwa University, Shoufeng, Hualien 974, Taiwan<sup>§</sup>Department of Physical Chemistry and Molecular Modeling, Opole University, 45-052 Opole, Poland

## S Supporting Information

**ABSTRACT:** The bimolecular gas-phase reaction of ground-state atomic silicon ( $\text{Si}$ ;  $^3\text{P}$ ) with disilane ( $\text{Si}_2\text{H}_6$ ;  $^1\text{A}_{1g}$ ) was explored under single-collision conditions in a crossed molecular beam machine at a collision energy of  $21 \text{ kJ mol}^{-1}$ . Combined with electronic structure calculations, the results suggest the formation of  $\text{Si}_3\text{H}_4$  isomer(s) along with molecular hydrogen via indirect scattering dynamics through  $\text{Si}_3\text{H}_6$  collision complex(es) and intersystem crossing from the triplet to the singlet surface. The nonadiabatic reaction dynamics can synthesize the energetically accessible singlet  $\text{Si}_3\text{H}_4$  isomers in overall exoergic reaction(s) ( $-93 \pm 21 \text{ kJ mol}^{-1}$ ). All reasonable reaction products are either cyclic or hydrogen-bridged suggesting extensive isomerization processes from the reactants via the initially formed collision complex(es) to the fragmenting singlet intermediate(s). The underlying chemical dynamics of the silicon–disilane reaction are quite distinct from the isovalent carbon–ethane system that does not depict any reactivity at all, and open the door for an unconventional gas phase synthesis of hitherto elusive organosilicon molecules under single-collision conditions.



For almost a century, Langmuir's concept of isoelectronicity<sup>1,2</sup> has been instrumental in the establishment of contemporary concepts of chemical structure and bonding. Specific interest has been devoted to contrasting the chemistries of carbon and silicon.<sup>3–5</sup> With both carbon and silicon located in main group 14, both atoms have each four valence electrons and hence fulfill the concept of isovalency. However, the chemical bonding and molecular structures can be quite different for carbon and silicon, as evident from the linear acetylene ( $\text{HCCH}$ ; I)<sup>6</sup> strongly contrasting the dibridged disilyne species ( $\text{Si}(\text{H}_2)_2$ ; III), which represents the global minimum of the  $\text{Si}_2\text{H}_2$  potential energy surface (PES) (Scheme 1).<sup>7,8</sup> Therefore, silicon hydrides have been exploited as benchmarks to understand not only the similarities but also the differences in the chemical bonding and molecular structures compared with their isovalent hydrocarbon counterparts.<sup>9–11</sup>

Whereas the  $\text{C}_2\text{H}_2$  and  $\text{Si}_2\text{H}_2$  surfaces have been explored both experimentally and computationally,<sup>6,11–13</sup> the next higher homologues in this series,  $\text{Si}_3\text{H}_4$ , have escaped any experimental identification to date. This is in sharp contrast with the isovalent  $\text{C}_3\text{H}_4$  isomers with methylacetylene (VII) being the global minimum only  $5 \text{ kJ mol}^{-1}$  below the energy of allene (VIII);<sup>14</sup> three singlet carbenes (X, XI, XII) have significantly higher energies of up to  $273 \text{ kJ mol}^{-1}$  above methylacetylene (Scheme 2).<sup>9,14</sup> The inability in synthesizing any  $\text{Si}_3\text{H}_4$  isomer (Scheme 2; XIII–XIV) showcases the difficulties of silicon to form silicon–silicon double bonds due to the size of the silicon

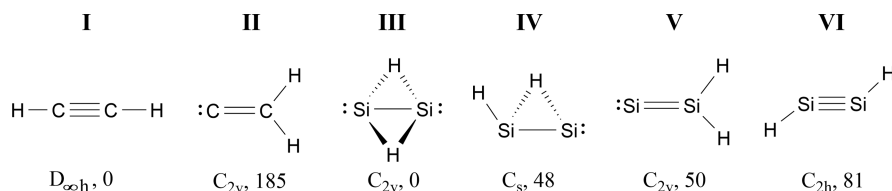
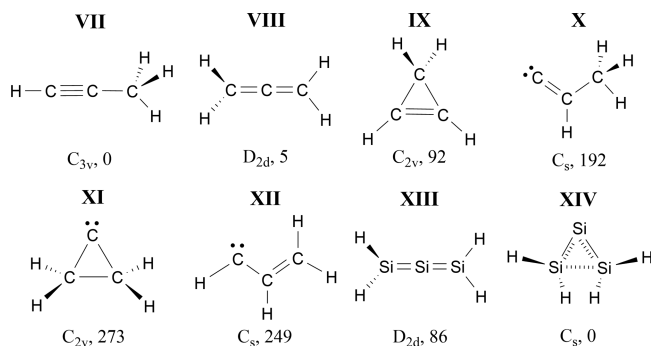
atom that precludes an atomic p orbital from approaching sufficiently close to a second silicon atom to form  $\pi$  bonds. Electronic structure calculations, however, suggest that various  $\text{Si}_3\text{H}_4$  isomers like XIII and XIV are kinetically stable.<sup>9,15</sup> In addition to the structures equivalent to  $\text{C}_3\text{H}_4$ , multiple  $\text{Si}_3\text{H}_4$  isomers have been located within  $100 \text{ kJ mol}^{-1}$  including hydrogen-bridged isomers, whose carbon counterparts do not exist. Most interestingly, a highly bent  $\text{H}_2\text{SiSiSiH}_2$  structure with a delocalized  $\pi$ -system over the three silicon atoms (XIV) was found residing  $86 \text{ kJ mol}^{-1}$  below the carbon analogue trisilaallene (XIII), which was characterized only as a second-order saddle point.<sup>9,16</sup> Therefore, a replacement of carbon by isovalent silicon leads to novel molecules, whose isovalent carbon counterparts do not always exist. Interestingly, electronic structure calculations predict that the substitution of hydrogen atoms in the bent trisilaallene ( $\text{H}_2\text{SiSiSiH}_2$ ; XIV) by bulky and electropositive groups possessing  $\sigma$ -donor and  $\pi$ -acceptor character restores the  $\text{Si}=\text{Si}=\text{Si}$  bond linearity from an acute angle of  $\sim 70^\circ$ .<sup>15,17,18</sup> Recently, thermally stable, crystalline compounds with formally sp-hybridized silicon atoms have been synthesized via substitution of the hydrogen atoms by bulky groups (XV, XVI; Scheme 3).<sup>17,18</sup> These results highlight the striking differences in molecular structure and

Received: November 19, 2016

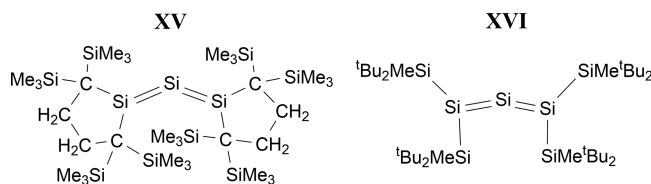
Accepted: December 13, 2016

Published: December 13, 2016



Scheme 1. Lewis Structures of Distinct  $C_2H_2$  (I, II) and  $Si_2H_2$  Isomers (III–VI)<sup>a</sup><sup>a</sup>Point groups and relative energies (kJ mol<sup>−1</sup>) with respect to the most stable isomer are also given.Scheme 2. Structures of  $C_3H_4$  Isomers (VII–XII) and Selected  $Si_3H_4$  Isomers (XIII, XIV)<sup>a</sup><sup>a</sup>Point groups and relative energies (kJ mol<sup>−1</sup>) with respect to the most stable isomer are also given. XIII represents a transition state.

Scheme 3. Structures of Isolated Trisilaallene-Based Compounds with Si=Si=Si Angles of 136°(XV) and 164°(XVI)



bonding of carbon hydrides versus silicon hydrides, thus emphasizing the need to synthesize higher silicon hydrides experimentally to gain innovative insights into the exotic chemical bonding of carbon versus silicon and to supply basic concepts on chemical reactivity and bond-cleavage processes of silicon-bearing molecules.

We present the results of a crossed molecular beam reaction of ground-state atomic silicon (Si; <sup>3</sup>P) with disilane (Si<sub>2</sub>H<sub>6</sub>; <sup>1</sup>A<sub>1g</sub>) under single collision conditions to synthesize for the very first time free Si<sub>3</sub>H<sub>4</sub> isomers in the gas phase via nonadiabatic reaction dynamics. These results shed light on an exotic silicon chemistry and puzzling chemical dynamics of atomic silicon, which are very different compared with the isovalent carbon systems.

The reactive scattering signal was recorded at mass-to-charge ratios (*m/z*) of 91 to 87 to probe potential adducts along with atomic and molecular hydrogen loss pathways. Accounting for the natural abundances of silicon (<sup>30</sup>Si (3.10%), <sup>29</sup>Si (4.67%), <sup>28</sup>Si (92.23%)), and carbon (<sup>13</sup>C (1.1%), <sup>12</sup>C (98.9%)), no signal was detected at *m/z* 91 and 90, indicating the absence of adducts (<sup>29</sup>Si<sup>28</sup>Si<sub>2</sub>H<sub>6</sub><sup>+</sup>/<sup>28</sup>Si<sub>3</sub>H<sub>6</sub><sup>+</sup>) and the atomic hydrogen loss channel (<sup>29</sup>Si<sup>28</sup>Si<sub>2</sub>H<sub>5</sub><sup>+</sup>/<sup>30</sup>Si<sup>28</sup>Si<sub>2</sub>H<sub>5</sub><sup>+</sup>). However, signal was observed at *m/z* 89 and 88. Ion counts at *m/z* 89 could arise from the atomic hydrogen loss pathway (<sup>28</sup>Si<sub>3</sub>H<sub>5</sub><sup>+</sup>) or from the

molecular hydrogen emission channel (<sup>29</sup>Si<sup>28</sup>Si<sub>2</sub>H<sub>4</sub><sup>+</sup>); signal at *m/z* 88 could be attributed to the molecular hydrogen elimination pathway forming <sup>28</sup>Si<sub>3</sub>H<sub>4</sub> isomer(s). Considering that the time-of-flight (TOF) spectra at *m/z* 89 and 88 are superimposable after scaling, signals at *m/z* 89 and 88 originate from ionized <sup>29</sup>Si<sub>3</sub>H<sub>4</sub> and <sup>28</sup>Si<sub>3</sub>H<sub>4</sub> (hereafter: Si<sub>3</sub>H<sub>4</sub>), respectively. Finally, signal at *m/z* 87 stems from dissociative electron impact fragmentation of the Si<sub>3</sub>H<sub>4</sub> product to Si<sub>3</sub>H<sub>3</sub><sup>+</sup>. Therefore, the laboratory data alone provide evidence of the existence of the molecular hydrogen loss pathway forming Si<sub>3</sub>H<sub>4</sub> isomers in the reaction of ground-state atomic silicon with disilane. The associated laboratory angular distribution obtained at *m/z* 88 (<sup>28</sup>Si<sub>3</sub>H<sub>4</sub><sup>+</sup>) depicts a distribution maximum close to the center-of-mass (CM) angle of 51.9 ± 1.0° and spans a scattering range of ~45° (Figure 1). These results indicate a complex-forming reaction mechanism (indirect scattering dynamics) involving Si<sub>3</sub>H<sub>6</sub> intermediate(s).

The final objectives of our study are not only to extract the molecular formula of the reaction product (Si<sub>3</sub>H<sub>4</sub>) but also to untangle the structure(s) of the isomer(s) along with the formation mechanism(s) of the exotic organosilicon molecules. To accomplish this goal, it is important to acquire information on the chemical dynamics. This is achieved by exploiting a forward-convolution routine,<sup>19</sup> which transforms the laboratory data (TOF spectra, laboratory angular distribution) of the Si<sub>3</sub>H<sub>4</sub> product(s) detected via its parent ion at *m/z* 88 into the CM reference frame. This approach yields two “best-fit” CM functions: the translational energy flux distribution *P*(*E*<sub>T</sub>) and the angular flux distribution *T*(*θ*) (Figure 2). A close inspection of the CM translational energy flux distribution, *P*(*E*<sub>T</sub>), reveals a maximum translational energy (*E*<sub>max</sub>) of 114 ± 19 kJ mol<sup>−1</sup>. For molecules born without rovibrational excitation, *E*<sub>max</sub> represents the sum of the collision energy plus the reaction exoergicity. Therefore, a subtraction of the collision energy from *E*<sub>max</sub> suggests that the reaction forming Si<sub>3</sub>H<sub>4</sub> plus H<sub>2</sub> is exoergic by 93 ± 20 kJ mol<sup>−1</sup>. Also, the *P*(*E*<sub>T</sub>) shows a broad distribution maximum from zero to ~20 kJ mol<sup>−1</sup>; this broad plateau suggests multiple exit channels upon unimolecular decomposition of the Si<sub>3</sub>H<sub>6</sub> complex forming Si<sub>3</sub>H<sub>4</sub> isomer(s) via molecular hydrogen elimination.<sup>20</sup> Finally, the CM angular flux distribution *T*(*θ*) depicts flux over the complete scattering range from 0 to 180°. The “best-fit” *T*(*θ*) results in a symmetric forward–backward scattered distribution, indicating the lifetime(s) of the decomposing complex(es) is(are) longer than its(their) rotational period(s).<sup>21</sup> Furthermore, the pronounced distribution maximum close to 90° suggests geometrical constraints upon decomposition of at least one Si<sub>3</sub>H<sub>6</sub> complex in which the molecular hydrogen is emitted perpendicularly to the rotational plane of the decomposing complex almost parallel to the total angular momentum vector.<sup>22</sup>

Possible Si<sub>3</sub>H<sub>4</sub> isomer(s) formed via the bimolecular reaction of ground-state atomic silicon with disilane can be revealed by

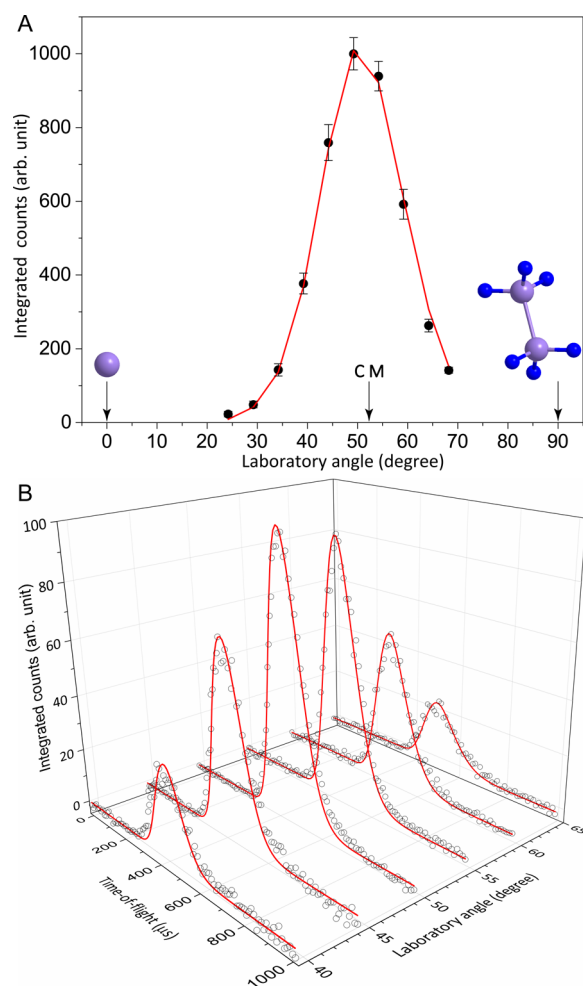


**Figure 1.** Laboratory angular distribution (A) and time-of-flight spectra (B) recorded at a mass-to-charge ratio 88 ( $\text{Si}_3\text{H}_4^+$ ) in the reaction of ground-state atomic silicon with disilane. The circles define the experimental data and the red lines represent the fitting based on the best-fit center-of-mass functions, as depicted in Figure 2. Errors with an uncertainty of  $\pm 1\sigma$  are indicated. Here CM arrow indicates the center-of-mass angle.

comparing the experimentally determined reaction energy ( $-93 \pm 20 \text{ kJ mol}^{-1}$ ) with the reaction energies obtained from our electronic structure calculations (Figure 3; Supporting Information). The geometries and relative energies of the triplet and singlet  $\text{Si}_3\text{H}_4$  isomers were explored via electronic structure calculations, as described in the Methods. In detail, our investigations indicate the existence of 10 triplet and 19 singlet  $\text{Si}_3\text{H}_4$  isomers. Among the triplet isomers, even the energetically most favorable isomer  $^3\text{p10}$  ( $-47 \pm 8 \text{ kJ mol}^{-1}$ ) does not correlate with the experimentally derived reaction energy of  $-93 \pm 20 \text{ kJ mol}^{-1}$ . Considering the singlet  $\text{Si}_3\text{H}_4$  surface, within the error limits, eight singlet isomers ( $^1\text{p8}$  to  $^1\text{p17}$ ), which are linked to reaction energies between  $-75 \pm 8$  and  $-97 \pm 8 \text{ kJ mol}^{-1}$ , can account for the experimentally determined reaction energy of  $-93 \pm 20 \text{ kJ mol}^{-1}$ . Therefore, we can conclude that because the reaction of ground-state atomic silicon with disilane starts on the triplet surface, but the energetically feasible product(s) ( $^1\text{p8}$  to  $^1\text{p17}$ ) along with molecular hydrogen both hold singlet ground states, at least one channel of the reaction must involve intersystem crossing and hence nonadiabatic reaction dynamics. A closer look at the

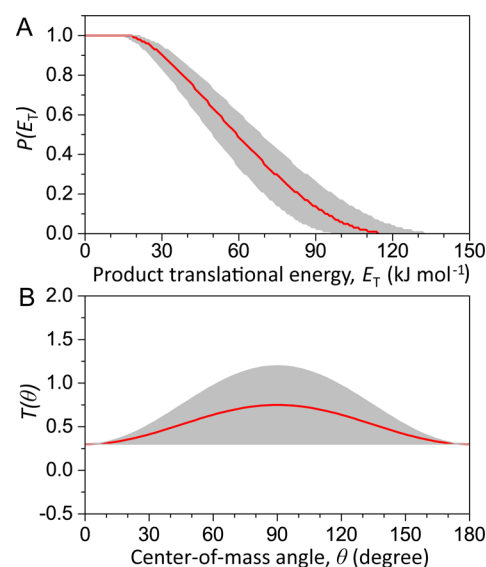


**Figure 2.** Center-of-mass translational energy flux distribution  $P(E_T)$  (A) and angular distribution  $T(\theta)$  (B) leading to the formation of the  $\text{Si}_3\text{H}_4$  molecules plus molecular hydrogen in the reaction of ground-state atomic silicon with disilane. Shaded areas indicate the acceptable upper and lower error limits of the fits. The red solid lines define the best-fit functions.

geometry of the reactants and potential products ( $^1\text{p8}$  to  $^1\text{p17}$ ) suggests that isomers  $^1\text{p8}$  to  $^1\text{p11}$ ,  $^1\text{p13}$ , and  $^1\text{p17}$  hold a single silyl group. Furthermore, all of those energetically accessible product isomers are cyclic holding a  $\text{Si}_3$  moiety except for  $^1\text{p9}$  and  $^1\text{p11}$ , which are cyclic structures associated with bridged hydrogen atom. Therefore, hydrogen migration(s) or isomerization via cyclization must be important steps in the reaction of ground-state silicon with disilane. Considering the complexity of this system (intersystem crossing, ten energetically accessible product isomers), a presentation of a complete singlet and triplet  $\text{Si}_2\text{H}_6$  surface along with the search for conical intersections is beyond the scope of this Letter but will be conducted in the future.

In conclusion, our investigation of the bimolecular gas-phase reaction of ground-state atomic silicon ( $\text{Si}; ^3\text{P}$ ) with disilane ( $\text{Si}_2\text{H}_6; ^1\text{A}_1\text{g}$ ) revealed indirect scattering dynamics via  $\text{Si}_3\text{H}_6$  collision complex(es) along with a facile formation singlet  $\text{Si}_3\text{H}_4$  isomer(s) involving intersystem crossing from the triplet to the singlet surface. These nonadiabatic reaction dynamics can lead to the formation of one (or more) singlet  $\text{Si}_3\text{H}_4$  isomers ( $^1\text{p8}$  to  $^1\text{p17}$ ) in overall exoergic reaction(s) ( $-93 \pm 20 \text{ kJ mol}^{-1}$ ). Both the broad distribution maximum of the CM translational energy distribution and the shape of the CM angular distribution suggest multiple exit channels, of which at least one pathway is likely barrierless, but the second mechanism could involve a tight exit transition state. In strong contrast, the isovalent carbon–ethane system shows no reactivity at all. Consequently, the isovalency of the silicon atom predicts an incorrect reactivity in this system. This finding strongly influences how we rationalize not only the chemical reactivity of silicon-containing systems but also the reaction mechanism, thermochemistry, and chemical bonding classifying the silicon–disilane system as a critical benchmark toward a detailed understanding of the formation of small (organo)silicon molecules. The comparison of the chemical behavior of silicon relative to carbon is fundamental to our understanding of



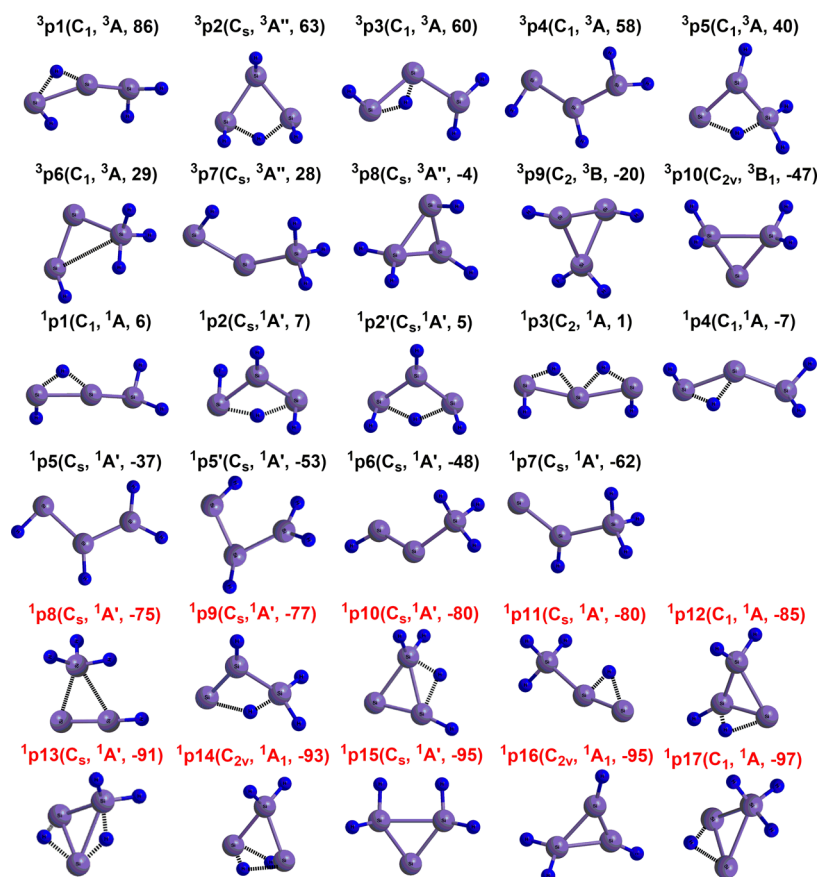


**Figure 3.** Computed structures of triplet ( $^3\text{p1-}^3\text{p10}$ ) and singlet ( $^1\text{p1-}^1\text{p17}$ )  $\text{Si}_3\text{H}_4$  isomers along with their point groups and symmetries of the electronic wave functions. The labels in red indicate the isomers that are energetically accessible under current experimental conditions. The energies are given in  $\text{kJ mol}^{-1}$  relative to the energies of the separated reactants.

chemistry and will affect how we explain chemical bonding involving silicon atoms and how we think about chemical structure in the future. Further experimental and theoretical studies of these systems under single-collision conditions are clearly warranted to fully uncover the unique reactivity of atomic silicon along with the formation of novel organosilicon molecules to gain a comprehensive understanding of their electronic structures, chemical bonding, and stability.

## METHODS

**Crossed Molecular Beam Experiments.** The reaction of atomic silicon ( $\text{Si}$ ;  $^3\text{P}$ ) with disilane ( $\text{Si}_2\text{H}_6$ ;  $^1\text{A}_g$ ) was investigated in a universal crossed molecular beam machine at the University of Hawaii at Manoa.<sup>23,24</sup> In the primary source chamber, a pulsed beam of neon-seeded silicon atoms was produced in situ by ablating a rotating silicon target by 266 nm photons from the output of a Spectra-Physics Quanta-Ray Pro 270 Nd:YAG laser operating at 30 Hz and power of  $9 \pm 1$  mJ per pulse. The ablated species were then seeded in neon ( $\text{Ne}$ ; 99.999%; Specialty Gases of America) carrier gas at a backing pressure of 4 atm released from a pulsed piezoelectric valve (Piezo Disk Translator P-286.23; Physik Instrumente) operated with a repetition rate of 60 Hz, a pulse width of 80  $\mu\text{s}$ , and a peak voltage of  $-400$  V. The pulsed beam of the silicon atoms passed through a skimmer and a four-slit chopper wheel rotating at 120 Hz; the chopper wheel selected a pulse of the silicon atom beam with a well-defined peak velocity ( $v_p$ ) and speed ratio ( $S$ ) of  $1390 \pm 14$   $\text{ms}^{-1}$  and  $2.8 \pm 0.2$ , respectively.

In the secondary chamber, a pulsed beam of disilane (99.998%, Voltaix) was prepared by a second piezoelectric valve operating at 60 Hz, a pulse width of 80  $\mu\text{s}$ , and a peak voltage of  $-400$  V with a backing pressure of 550 Torr; this resulted in a peak velocity and speed ratio of  $750 \pm 15$   $\text{ms}^{-1}$  and  $7.2 \pm 0.4$  for the disilane pulse. Because of the extreme flammability of disilane, we incorporated a nitrogen cold trap (Nor-Cal, Inc.) between the turbo molecular pump and roots roughing pump to trap disilane. After passing through the secondary skimmer, the pulsed disilane beam crossed perpendicularly with the beam of atomic silicon at a collision energy of  $21.0 \pm 0.8$   $\text{kJ mol}^{-1}$ ; the center-of-mass (CM) angle was calculated to be  $51.9 \pm 1.0^\circ$ . Note that the primary pulsed valve was triggered after 1872  $\mu\text{s}$  with respect to the time zero defined by the infrared diode mounted at the top of the chopper wheel, while the flash lamps of the ablation laser were fired 155  $\mu\text{s}$  after the primary pulse valve with Q-switch initiated 186  $\mu\text{s}$  after the flash lamp pulse to allow a maximum overlap of the laser pulse with the neon beam. The secondary pulsed valve was triggered 65  $\mu\text{s}$  prior to the primary pulsed valve due to the lower velocity of disilane. The 60 Hz repetition rate of pulsed valves and 30 Hz frequency of the ablation laser enable a “laser-on” minus “laser-off” subtraction to eliminate potential background. The reactively scattered products were mass-filtered after ionization utilizing a quadrupole mass filter and detected by a Daly type time-of-flight (TOF) detector housed in a rotatable, triply differentially pumped ultrahigh vacuum chamber ( $1 \times 10^{-11}$  Torr) after electron-impact ionization of the neutral products at an electron energy of 80 eV and an emission current of 2 mA.

This detector can be rotated within the plane defined by the primary and the secondary reactant beams, allowing recording of angular-resolved TOF spectra. At each angle, up to  $6 \times 10^5$  TOF spectra were accumulated to obtain good signal-to-noise ratios. The recorded TOF spectra were then integrated and normalized to the intensity of the TOF at the CM angle to extract the product angular distribution in the laboratory frame. To acquire information on the scattering dynamics, the laboratory data were then transformed from the laboratory into the CM reference frame utilizing a forward-convolution routine.<sup>19,20,25</sup> This iterative method employs a parametrized or point-form translational energy flux distribution,  $P(E_T)$ , and angular flux distribution,  $T(\theta)$ , in the CM frame. Laboratory TOF spectra as well as the angular distribution are calculated from the  $P(E_T)$  and  $T(\theta)$  functions and are averaged over a grid of Newton diagrams accounting for the apparatus functions, beam divergences, and velocity spreads. For the fitting, we considered a reactive scattering cross section of an  $E_c^{-1/3}$  energy dependence, where  $E_c$  defines the translational energy. This method is adopted within the line-of-center model for exoergic and barrierless entrance reactions dominated by long-range attractive forces.<sup>26</sup> In addition to the mass spectrometric detection, the spin states of silicon atoms were characterized utilizing laser-induced fluorescence (LIF).<sup>27,28</sup> Silicon atoms in their ground (triplet) and first excited (singlet) states were probed via the  $3p^2\ ^3P \rightarrow 3p4s\ ^3P$  and  $3p^2\ ^1D \rightarrow 3p4s\ ^1P$  transitions around 251 and 288 nm, respectively. The  $^3P$  ground state was detected for several  $j$  states. No signal was observable for the  $3p^2\ ^1D_2 \rightarrow 3p4s\ ^1P_1$  transition implying the absence of electronically excited silicon atoms (Si;  $^1D$ ) in the beam.

**Electronic Structure Calculations.** The reaction of ground-state atomic silicon (Si;  $^3P$ ) with disilane ( $Si_2H_6$ ;  $^1A_{1g}$ ) is also explored theoretically. Here geometries of possible triplet and singlet  $Si_3H_4$  isomers are optimized via density functional B3LYP<sup>29–32</sup>/cc-pVTZ and coupled cluster<sup>33–36</sup> CCSD/cc-pVTZ calculations. The completed basis set limits,<sup>37</sup> CCSD(T)/CBS energies, are obtained by extrapolating the CCSD(T)/cc-pVDZ, CCSD(T)/cc-pVTZ, and CCSD(T)/cc-pVQZ energies, with B3LYP/cc-pVTZ or CCSD/cc-pVTZ zero-point energy corrections. The accuracy of these CCSD(T)/CBS energies is expected to be within  $8\text{ kJ mol}^{-1}$ .<sup>38</sup> GAUSSIAN09 programs<sup>39</sup> are facilitated in density functional and coupled cluster calculations.

## ■ ASSOCIATED CONTENT

### ■ Supporting Information

The Supporting Information is available free of charge on the ACS Publications website at DOI: [10.1021/acs.jpclett.6b02710](https://doi.org/10.1021/acs.jpclett.6b02710).

Figure S1: Laser-induced fluorescence spectra for  $^3P$  and  $^1D$  states of atomic silicon. Table S1: Optimized Cartesian coordinates, rotational constants, and vibrational frequencies of  $H_2$  dissociation products for the Si +  $Si_2H_6$  reaction. Table S2: Coupled cluster CCSD(T)/CBS energies with B3LYP/cc-pVTZ zero-point energy corrections of  $H_2$  dissociation products for the title reaction. (PDF)

## ■ AUTHOR INFORMATION

### Corresponding Authors

\*R.I.K.: E-mail: [ralfk@hawaii.edu](mailto:ralfk@hawaii.edu). Tel: +1-808-956-5731.

\*A.H.H.C.: E-mail: [hhchang@mail.ndhu.edu.tw](mailto:hhchang@mail.ndhu.edu.tw). Tel: +886-03-863-3596.

### ORCID

Ralf I. Kaiser: 0000-0002-7233-7206

### Present Address

<sup>†</sup>B.B.D.: Department of Chemistry, Florida A&M University, Tallahassee, Florida 32307, USA.

### Notes

The authors declare no competing financial interest.

## ■ ACKNOWLEDGMENTS

The Hawaii group thanks the National Science Foundation (NSF) for support under award CHE-1360658. Computer resources at the National Center for High-Performance Computing of Taiwan were utilized in the calculations.

## ■ REFERENCES

- (1) Langmuir, I. The Arrangement of Electrons in Atoms and Molecules. *J. Am. Chem. Soc.* **1919**, *41*, 868–934.
- (2) Langmuir, I. Isomorphism, Isosterism and Covalence. *J. Am. Chem. Soc.* **1919**, *41*, 1543–1559.
- (3) Kaftory, M.; Kapon, M.; Botoshansky, M. *The Structural Chemistry of Organosilicon Compounds*; John Wiley & Sons, Inc.: New York, 1998.
- (4) Corey, J. Y. *Historical Overview and Comparison of Silicon with Carbon*; John Wiley & Sons, Inc.: New York, 1989.
- (5) Sheldrick, W. S. *Structural Chemistry of Organic Silicon Compounds*; John Wiley & Sons, Inc.: New York, 1989.
- (6) Chen, Y.; Jonas, D. M.; Kinsey, J.; Field, R. High Resolution Spectroscopic Detection of Acetylene–Vinylidene Isomerization by Spectral Cross Correlation. *J. Chem. Phys.* **1989**, *91*, 3976–3987.
- (7) Colegrove, B. T.; Schaefer, H. F., III Disilyne ( $Si_2H_2$ ) Revisited. *J. Phys. Chem.* **1990**, *94*, 5593–5602.
- (8) Jursic, B. S. Potential Energy Surface for  $H_2Si_2$  Isomer Explored with Complete Basis Set Ab Initio Method. *J. Mol. Struct.: THEOCHEM* **1999**, *459*, 221–228.
- (9) Kosa, M.; Karni, M.; Apeloig, Y. Trisilaallene and the Relative Stability of  $Si_3H_4$  Isomers. *J. Chem. Theory Comput.* **2006**, *2*, 956–964.
- (10) Gordon, M. S.; Bartol, D. Molecular and Electronic Structure of  $Si_3H_6$ . *J. Am. Chem. Soc.* **1987**, *109*, 5948–5950.
- (11) Yang, T.; Dangi, B. B.; Kaiser, R. I.; Chao, K.-H.; Sun, B.-J.; Chang, A. H. H.; Nguyen, T. L.; Stanton, J. F. Gas Phase Formation of the Disilavinylidene ( $H_2SiSi$ ) Transient. *Angew. Chem., Int. Ed.* **2016**, DOI: [10.1002/anie.201611107](https://doi.org/10.1002/anie.201611107).
- (12) Tanaka, T.; Hiramatsu, M.; Nawata, M.; Kono, A.; Goto, T. Reaction Rate Constant of Si Atoms with  $SiH_4$  Molecules in a RF Silane Plasma. *J. Phys. D: Appl. Phys.* **1994**, *27*, 1660.
- (13) Maier, G.; Reisenauer, H. P.; Glatthaar, J. Reactions of Silicon Atoms with Methane and Silane in Solid Argon: A Matrix-Spectroscopic Study. *Chem. - Eur. J.* **2002**, *8*, 4383–4391.
- (14) Kakkar, R.; Garg, R.; Chadha, P.  $C_3H_4$ : Density Functional (DFT) Study of Structures and Stabilities of Isomers. *J. Mol. Struct.: THEOCHEM* **2002**, *617*, 141–147.
- (15) Kosa, M.; Karni, M.; Apeloig, Y. How to Design Linear Allenic-Type Trisilaallenes and Trigermaallenes. *J. Am. Chem. Soc.* **2004**, *126*, 10544–10545.
- (16) Veszprémi, T.; Petrov, K.; Nguyen, C. T. From Silaallene to Cyclotrisilanylidene. *Organometallics* **2006**, *25*, 1480–1484.
- (17) Tanaka, H.; Inoue, S.; Ichinohe, M.; Driess, M.; Sekiguchi, A. Synthesis and Striking Reactivity of an Isolable Tetrasilyl-Substituted Trisilaallene. *Organometallics* **2011**, *30*, 3475–3478.
- (18) Ishida, S.; Iwamoto, T.; Kabuto, C.; Kira, M. A Stable Silicon-Based Allene Analogue with a Formally Sp-Hybridized Silicon Atom. *Nature* **2003**, *421*, 725–727.
- (19) Weiss, P. S. Ph. D. Thesis, University of California at Berkeley, Berkeley, CA, 1986.

- (20) Kaiser, R. I.; Le, T. N.; Nguyen, T. L.; Mebel, A. M.; Balucani, N.; Lee, Y. T.; Stahl, F.; Schleyer, P. v. R.; Schaefer, H. F., III A Combined Crossed Molecular Beam and Ab Initio Investigation of  $C_2$  and  $C_3$  Elementary Reactions with Unsaturated Hydrocarbons - Pathways to Hydrogen Deficient Hydrocarbon Radicals in Combustion Flames. *Faraday Discuss.* **2001**, *119*, 51–66.
- (21) Miller, W. B.; Safron, S. A.; Herschbach, D. R. Exchange Reactions of Alkali Atoms with Alkali Halides: A Collision Complex Mechanism. *Discuss. Faraday Soc.* **1967**, *44*, 108–122.
- (22) Kaiser, R. I.; Parker, D. S. N.; Zhang, F.; Landera, A.; Kislov, V. V.; Mebel, A. M. PAH Formation under Single Collision Conditions: Reaction of Phenyl Radical and 1,3-Butadiene to Form 1,4-Dihydronaphthalene. *J. Phys. Chem. A* **2012**, *116*, 4248–4258.
- (23) Gu, X.; Kaiser, R. I. Reaction Dynamics of Phenyl Radicals in Extreme Environments: A Crossed Molecular Beam Study. *Acc. Chem. Res.* **2009**, *42*, 290–302.
- (24) Gu, X. B.; Guo, Y.; Zhang, F. T.; Mebel, A. M.; Kaiser, R. I. Reaction Dynamics of Carbon-Bearing Radicals in Circumstellar Envelopes of Carbon Stars. *Faraday Discuss.* **2006**, *133*, 245–275.
- (25) Vernon, M. F. Ph.D. Thesis, University of California at Berkeley, Berkeley, CA, 1983.
- (26) Levine, R. D.; Bernstein, R. B.; Lee, Y. T. Molecular Reaction Dynamics and Chemical Reactivity. *Phys. Today* **1988**, *41*, 90.
- (27) Nozaki, Y.; Kongo, K.; Miyazaki, T.; Kitazoe, M.; Horii, K.; Umamoto, H.; Masuda, A.; Matsumura, H. Identification of Si and SiH in Catalytic Chemical Vapor Deposition of  $SiH_4$  by Laser Induced Fluorescence Spectroscopy. *J. Appl. Phys.* **2000**, *88*, 5437–5443.
- (28) Maksyutenko, P.; Parker, D. S.; Zhang, F.; Kaiser, R. I. An LIF Characterization of Supersonic BO ( $X^2\Sigma^+$ ) and CN ( $X^2\Sigma^+$ ) Radical Sources for Crossed Beam Studies. *Rev. Sci. Instrum.* **2011**, *82*, 083107.
- (29) Becke, A. D. Density-functional Thermochemistry. I. The Effect of the Exchange-Only Gradient Correction. *J. Chem. Phys.* **1992**, *96*, 2155–2160.
- (30) Becke, A. D. Density-functional Thermochemistry. II. The Effect of the Perdew-Wang Generalized-Gradient Correlation Correction. *J. Chem. Phys.* **1992**, *97*, 9173–9177.
- (31) Becke, A. D. Density-functional Thermochemistry. III. The Role of Exact Exchange. *J. Chem. Phys.* **1993**, *98*, 5648–5652.
- (32) Lee, C.; Yang, W.; Parr, R. G. Development of the Colle-Salvetti Correlation-Energy Formula into a Functional of the Electron Density. *Phys. Rev. B: Condens. Matter Mater. Phys.* **1988**, *37*, 785.
- (33) Purvis, G. D., III; Bartlett, R. J. A Full Coupled-Cluster Singles and Doubles Model: The Inclusion of Disconnected Triples. *J. Chem. Phys.* **1982**, *76*, 1910–1918.
- (34) Hampel, C.; Peterson, K. A.; Werner, H.-J. A Comparison of the Efficiency and Accuracy of the Quadratic Configuration Interaction (QCISD), Coupled Cluster (CCSD), and Brueckner Coupled Cluster (BCCD) Methods. *Chem. Phys. Lett.* **1992**, *190*, 1–12.
- (35) Knowles, P. J.; Hampel, C.; Werner, H.-J. Coupled Cluster Theory for High Spin, Open Shell Reference Wave Functions. *J. Chem. Phys.* **1993**, *99*, 5219–5227.
- (36) Deegan, M. J.; Knowles, P. J. Perturbative Corrections to Account for Triple Excitations in Closed and Open Shell Coupled Cluster Theories. *Chem. Phys. Lett.* **1994**, *227*, 321–326.
- (37) Peterson, K. A.; Woon, D. E.; Dunning, T. H., Jr Benchmark Calculations with Correlated Molecular Wave Functions. IV. The Classical Barrier Height of the  $H + H_2 \rightarrow H_2 + H$  Reaction. *J. Chem. Phys.* **1994**, *100*, 7410–7415.
- (38) Peterson, K. A.; Dunning, T. H., Jr Intrinsic Errors in Several *ab initio* Methods: The Dissociation Energy of  $N_2$ . *J. Phys. Chem.* **1995**, *99*, 3898–3901.
- (39) Frisch, M. J.; Trucks, G. W.; Schlegel, H. B.; Scuseria, G. E.; Robb, M. A.; Cheeseman, J. R.; Scalmani, G.; Barone, V.; Mennucci, B.; Petersson, G. A. *Gaussian 09*, Revision D. 01; Gaussian: Wallingford, CT, 2009.